Chapter 6. Comprehensive biological evaluation protocols of selected compounds for their mechanism of action, efficacy and safety.

6.1 Molecular docking methodology for docking studies of compounds with ME3

6.1.1 Ligand Structure Preparation

The 3D structures of the ligands were built using Schrödinger Maestro (version 12.1.013, MMshare Version 4.7.013, release 2019-3, Platform Linux-x86_64) and prepared by LigPrep module using OPLS_2005 force field. All possible low energy ionization, tautomeric and stereoisomeric stereoisomers were generated within the pH of 7.0 ± 0.5 (which corresponds to the physiological conditions) range.

6.1.2 Protein structure preparation

The 3D structure of human malic enzyme 3 (ME3) was not available in the Protein Data Bank (PDB). The efforts to get ME3 co-crystal structure with inhibitor resulted in ME3 co-crystallized with oxalate (resolution: 1.8 Å). Using this crystal structure, in-house structure-based drug design activities were initiated. Protein structure was prepared using Protein Preparation Wizard tool implemented in Maestro. The right bond orders were assigned, hydrogen atoms were added to the protein and all the water molecules were deleted. ProtAssign utility was employed for the optimization of hydroxyl group orientation, amide groups of Asn and Gln, and charged state of His residues. The final restrained minimization using OPLS_2005 force field[32] was performed with a cut-off point until the average Root Mean Square Deviation (RMSD) of the hydrogen atoms reached 0.3 Å, leaving heavy atoms in place.

6.1.3 Grid Generation and GLIDE Docking

Since crystallized ME3 enzyme was in closed form, binding pocket was too small for the tool and designed ligand molecules to fit appropriately, therefore Induced Fit Docking (IFD) approach was adopted to generate the protein ligand complex suitable for defining the grid and to initiate molecular docking study. For the docking of tool compound **A** using IFD, grid box was defined by selecting centroid of co-crystallized inhibitor oxalate and box size was set to dock ligands length ≤ 20 Å. Residues refinement was set to 7 Å, and standard protocol with Extra Precision (XP) was utilized for the docking. In order to obtain optimal grid suitable for molecular docking, interaction grids were generated for each of the 10 IFD output poses with the help of Receptor Grid Generation Wizard of GLIDE.[33] Validation of docking protocol and binding mode is a very crucial step for the extrapolation of docking results to the binding

affinity. As per the in-house biochemical activity data, compound **A** showed similar SAR in both ME1 and ME3. Therefore, compound **A** and its analogues reported by Zhang *et al.*[20] were docked in different grids to understand the Structure Activity Relationship (SAR) on the basis of binding modes, and the grid explaining the differences in the ME3 biochemical activity was finalized for docking of designed molecules. Docking of all the ligands performed at XP mode with OPLS_2005 force field. Number of poses generated for each ligand were set to 100 (while keeping all the parameters at their default values). Docking poses were critically evaluated for the correct binding mode and its consistency as well as intermolecular interactions with the key residues of ME3 oxalate binding site.

6.2 *in vitro* screening protocols for screening of compounds in ME isoforms and PDAC cell lines

6.2.1 *in vitro* enzymatic assay

Malic enzymes catalyze the oxidative decarboxylation of malate to pyruvate with conversion of the co-factor β-NAD+/ NADP+ to β-NADH/ NADPH. In a fluorescence based assay, a coupled reaction is set up wherein an enzyme, Diaphorase, utilizes NADH/NADPH generated by malic enzymes, to convert the dye resazurin to a fluorescent molecule resorufin. Resorufin has a characteristic fluorescence with excitation/emission at 540/600 nm.[23] The intensity of the Resorufin fluorescence is measured which is directly proportional to the activity of malic enzymes.

The enzyme activity inhibition assay was set up in a 200 µL final reaction volume in a 96-well plate. As per the experimental design, 2 µL of the compounds at 100x the desired concentration, in DMSO, were added to the respective wells with 178 µL of assay buffer (Refer **Table 6.1**). The plate was incubated on a plate shaker at room temperature for 15 minutes, protected from light. The well contents were gently mixed by adding 10µL of respective human malic enzyme (ME1/ME2/ME3), and the plate was incubated on the plate shaker at room temperature for another 5 minutes, protected from light. Suitable 'enzyme only' and 'no enzyme' controls were included in the experiment. The enzymatic reaction was started by adding 10µL of 2mM β-NAD+/ NADP+. The reaction was gently mixed and the plate was initially left on a shaker at room temperature for ~5 minutes, protected from light. Later, the plate was incubated without shaking at room temperature for 2 hours. At the end of 2 hours, the fluorescence of the wells was measured at excitation 540nm and emission 600nm. The % enzyme activity of the compounds is obtained by normalizing the data with enzyme only (100%) and no enzyme controls (0%) using GraphPad Prism software 9.02.

Table 6.1: *in vitro* biochemical assays for studying the effect of NCEs on malic enzyme activity

Enzyme	Substrate	Assay buffer	Incubation time
Recombinant Human ME3 (26-604) – His-tagged	3mM L – Malate, 50µM β-NADP+	50mM Tris-HCl, pH7.4, containing 10mM MnCl2, 50µM Resazurin and 0.025mg/ml Diaphorase, each at final concentrations	3 hours
Recombinant Human ME2 (Full length) – His tagged	7mM L – Malate, 100µM β-NAD+		2 hours
Recombinant Human ME1 (Full length) – His tagged	2mM L – Malate, 15µM β-NADP+		2 hours

6.2.2 *in vitro* BxPC-3 cell growth inhibition assay:

6.2.2.1 Cell Culture:

The pancreatic cancer cell line, BxPC-3 was obtained from the American Type Culture Collection (ATCC). BxPC-3 cells were cultured in RPMI- 1640 (Himedia, India) medium supplemented with 10% FBS (Gibco, USA), 2 mM L-glutamine (Sigma), 100 U/mL penicillin G and 100 µg/mL streptomycin (Sigma). Cell line was maintained in a humidified atmosphere with 5% CO_2 at 37˚C.

6.2.2.2 Cell growth inhibition assay:

Cell viability was determined using the CellTiter-Glo luminescence assay (Promega, USA) according to the manufacturer's suggested protocol. Luminescent signals were detected using a TECAN M1000 PRO microplate reader (TECAN, Switzerland). Briefly, BxPC-3 cells were seeded at a density of 2000 cells per well in 100 µl of RPMI-1640 growth medium supplemented with 10% FBS in a 96-well plate and were allowed to grow overnight. Next day, cells were treated in duplicate with vehicle (0.5% DMSO) or various concentrations of compounds and incubated for 72 h. Cell proliferation/viability was measured using the CellTiter-Glo luminescence assay. Luminescence values were calculated to percentage growth inhibition relative to the vehicle control (0.5% DMSO). IC_{50} was calculated using statistical analysis Log (inhibitor) vs % growth inhibition – variable slope (four parameters) using GraphPad Prism software 9.02.

6.2.3 *in vitro* Hs766T cell growth inhibition assay:

6.2.3.1 Cell Culture:

The pancreatic cancer cell line, Hs766T was obtained from the American Type Culture Collection (ATCC). Hs766T cells were cultured in DMEM (Himedia, India) medium supplemented with 10% FBS (Gibco, USA), 100 U/mL penicillin G and 100 µg/mL streptomycin (Sigma). Cell line was maintained in a humidified atmosphere with 5% CO_2 at 37˚C.

6.2.2.2 Cell growth inhibition assay:

Cell viability was determined using the CellTiterGlo® luminescence assay (Promega, USA) according to the manufacturer's protocol. Luminescence signals were detected using Varioskan® microplate reader (Thermo Fisher). Briefly, Hs766T cells were seeded at a density of 2000 cells/100 µl per well, in a 96-well plate and were allowed to grow overnight. Next day, cells were treated in duplicate with vehicle (0.5% DMSO) or various concentrations of compounds and incubated for 96h. Luminescence values were converted to percentage growth inhibition relative to the vehicle control (0.5% DMSO). IC_{50} was calculated using statistical analysis log [inhibitor] vs % growth inhibition – variable slope (four parameters), in GraphPad Prism software 9.04. A similar assay was performed for longer incubation period i.e. 2 weeks, with an initial seeding density of 500 cells/well. The compound in the growth media for long term assay was replenished every 3rd day until the termination of the assay.

6.3 Mechanism of ME3 inhibition studies for compounds 31 and 64.

6.3.1 *in vitro* enzymatic assay to investigate the mode of ME3 inhibition

In order to understand the mode of inhibition of compounds **31** and **64**; Their effects on Michaelis Menten kinetic parameters of hME3 enzymatic reaction were studied.[34] Briefly, the reaction velocity was continuously monitored at varying concentrations of the substrate, in presence of three different concentrations of the compound. Since the malic enzymes have two substrates i.e. L-malate and $NADP^+$, two separate substrate saturation experiments were performed. The first experiment was performed with varying concentrations of L-malate and saturating concentration of β-$NADP^+$ whereas the second one with varying concentrations of β-$NADP^+$ and saturating concentration of L-malate. The effect of compound doses on K_M of each substrate and maximum velocity of the reaction (V*max*), was studied, using Lineweaver-Burk's method of enzyme kinetics analysis.31 The assay was set up in a 96-well plate with 200µl of final reaction volume. The enzymatic reaction was started by adding β-$NADP^+$ to achieve its desired final concentration in the reaction (**Table 6.2**). The reaction progress was

continuously monitored for 10 minutes by measuring the absorbance at 340nm. The absorbance values at each time point were converted to reaction velocity units and expressed in terms of product formation per unit time (β-NADPH, μM/min).

Table 6.2: Concentrations of enzyme and substrates used in experiment

Enzyme	Substrate	Assay buffer
2 nM of Recombinant Human ME3 (26-604) – His-tagged	Expt-1: 0.4 to 50 mM L – Malate, 1 mM β-$NADP^+$ Expt-2: 20 mM L – Malate, 0.04 to 0.5 mM β-NADP	50 mM Tris-HCl, pH 7.4, containing 10 mM $MnCl_2$

6.3.2 Mode of inhibition study for compound 31

6.3.2.1 Experiment-1: Malate saturation curve for compound 31

Michaelis Menten plot

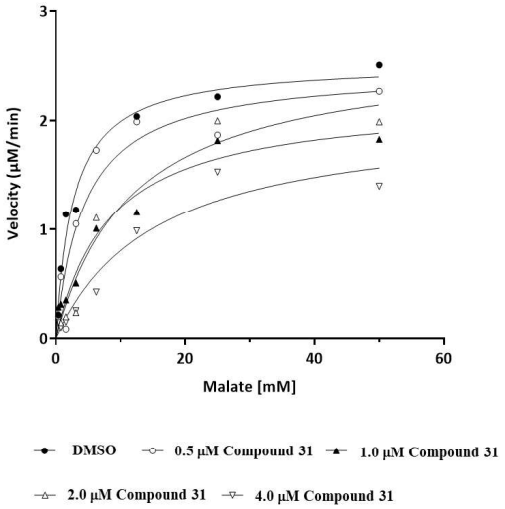

Lineweaver-Burk Plot

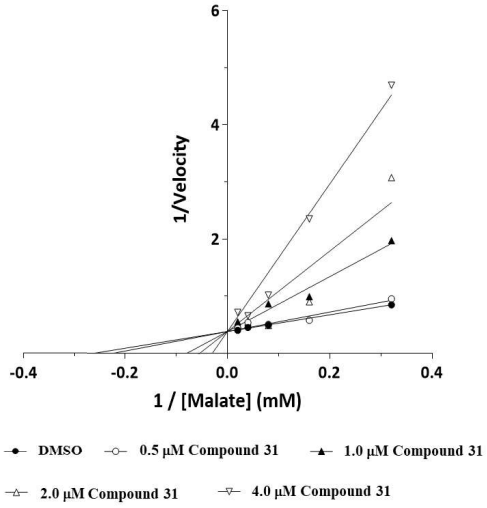

6.3.2.2 Experiment-2: $NADP^+$ saturation curve for compound 31

Michaelis Menten plot

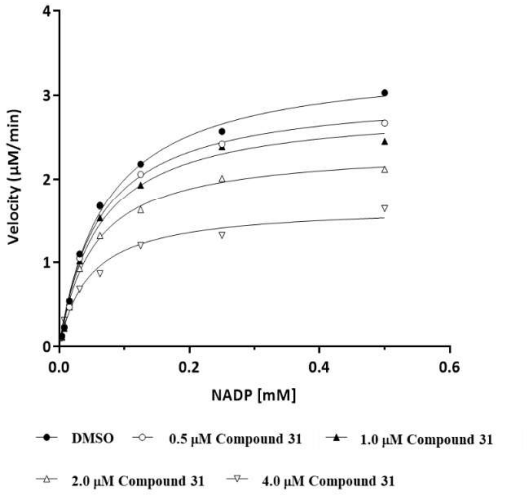

Lineweaver-Burk Plot

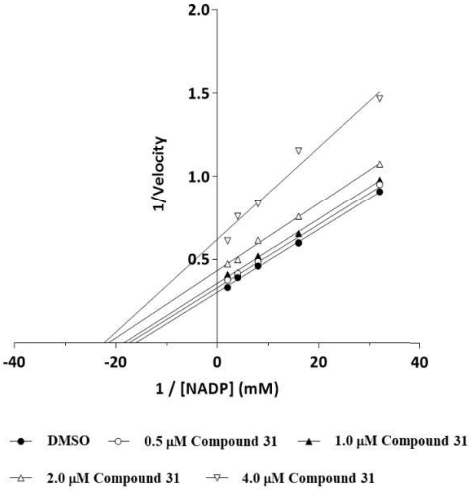

6.3.2.3 Analysis of K_M and V_{max} for compound 31

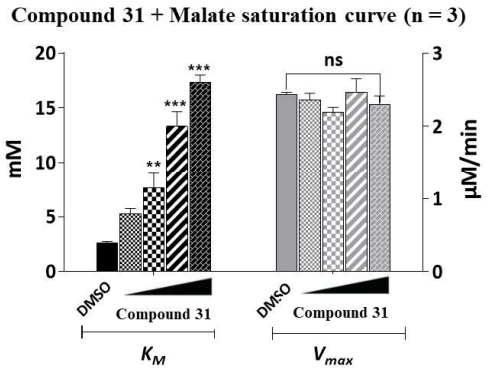

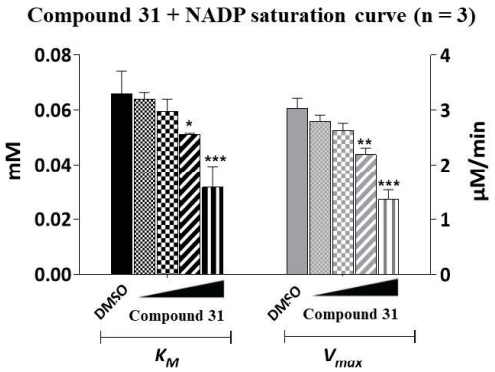

After analysis of these double-reciprocal plots it was concluded that compound **31** was a competitive inhibitor referring to L-malate and was an uncompetitive inhibitor with respect to $NADP^+$.

6.3.3 Mode of inhibition study for compound 62

6.3.3.1 Experiment-1: Malate saturation curve for compound 62

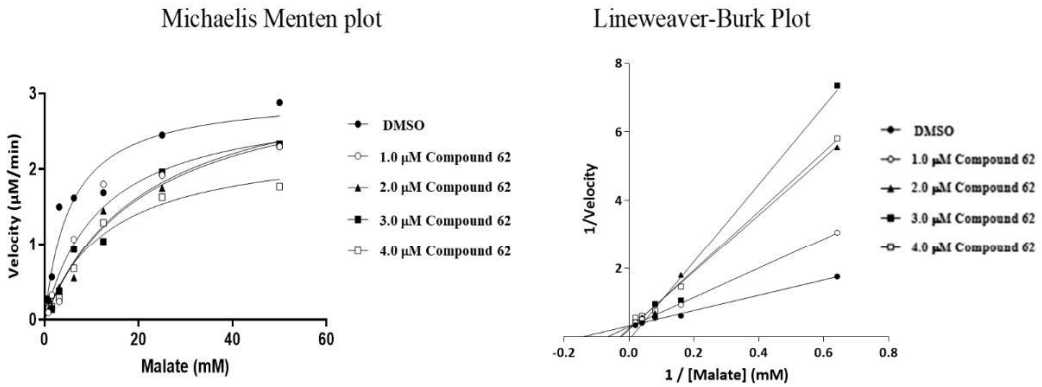

6.3.3.2 Experiment-2: $NADP^+$ saturation curve for compound 62

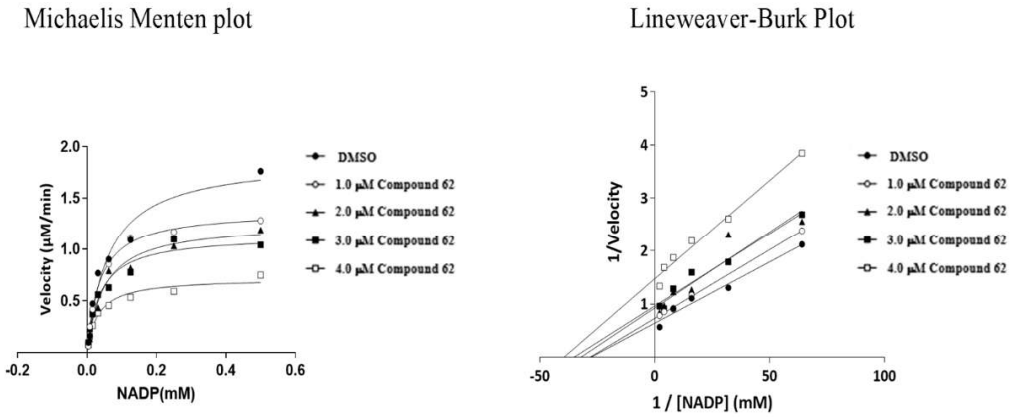

6.3.3.3 Analysis of K_M and V_{max} for compound 62

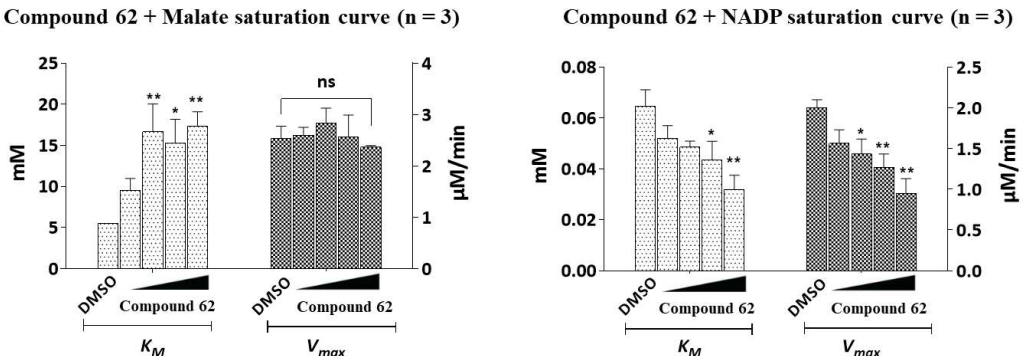

After analysis of these double-reciprocal plots it was concluded that compound **62** was a competitive inhibitor referring to L-malate and was an uncompetitive inhibitor with respect to $NADP^+$.

6.4 Target (ME3) engagement studies for compound 31 and 62 in BxPC-3 cells

6.4.1 CETSA (Cellular Thermal Shift Assay) for compound 31 with BxPC-3 live cells

6.4.1.1 Melt-curve analysis

In order to ascertain the target (ME3) engagement by compound **31**, a Cell based Thermal Shift Assay (CETSA) was performed using BxPC-3 live cells, in presence of compound **31.** Based on the experimental methods published by Jafari et al (2014)[24] and Langebäck et al (2019)[25]. Briefly, 5 x 10^5 cells were pre-incubated with 100 µM of compound **31** for 24 hours, at 37 ºC in 5% CO_2. Next day, 0.1 x 10^5 of cells exposed to compound **31** were dispensed into individual sample tubes followed by their exposure to a range of high temperatures (~ 45 to 85 ºC). All the samples were then analyzed, for checking the temperature induced effects on ME3 protein stability, by SDS-PAGE and western blotting, using a specific antibody against ME3.

The result indicated that that ME3 showed a resistance to temperature induced degradation upon binding with compound **31**. A Tm shift of nearly 5 ºC was observed with live BxPC-3 cells in presence of compound **31** as a proof for its target engagement with ME3 protein (**Figure 6.1**).

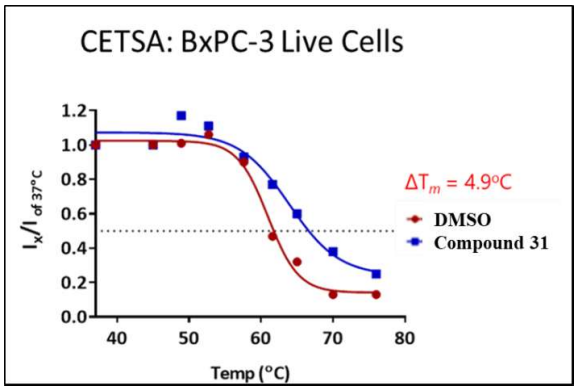

Figure 6.1: Melt-curve analysis for compound 31 with ME3 in live BxPC-3 cells.

6.4.1.2 Isothermal Dose Response Fingerprint (ITDRF) study

A similar experiment was performed by pre-incubating various concentrations of compound **31** with BxPC-3 live cells at 37 ºC in 5% CO_2, for 24 hours; and then exposing them to 67 ºC, (a median temperature in the ΔTm range, at which ME3 bound to 100 µM of compound **31** was found to be stable).

After performing the western blot analysis, it was found that ME3 from live cells, resisted temperature induced degradation at 67 ºC, in a concentration dependent manner of compound **31** (**Figure 6.2**). The EC_{50} of compound **31** for thermostabilization of ME3 was found to be ~3 µM (**Figure 6.2**).

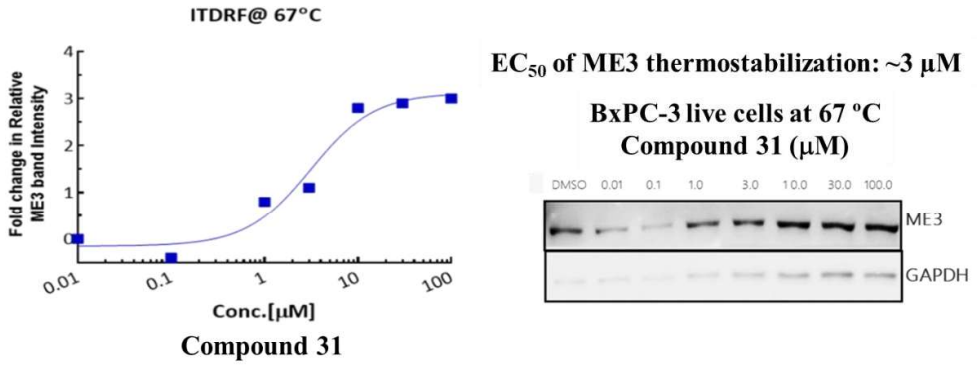

Figure 6.2: Isothermal Dose Response Fingerprint (ITDRF) with BxPC-3 live cells

6.4.2 CETSA (Cellular Thermal Shift Assay) for compound 62 with BxPC-3 cells

6.4.2.1 Melt-curve analysis

In order to ascertain the target (ME3) engagement by compound **62**, a cell based thermal shift assay was performed using the BxPC-3 cell lysate ($ME2^{-/-}$pancreatic cancer cell line). Based on the experimental methods published by Jafari *et. al.* (2014)[24] and Langebäck *et. al.* (2019)[25], the lysates prepared from BxPC-3 cells were pre-incubated with 100 µM of compound **62** for 30 min at room temperature; followed by exposure to a range of high temperatures (~ 50 to 80 ºC). Samples were then analyzed for checking the temperature induced effects on ME3 protein stability by SDS-PAGE and western blotting, using a specific antibody against ME3.

It was found that ME3 showed a resistance to temperature induced degradation upon binding with compound **62**. A T_m shift of nearly 5 ºC was observed with BxPC-3 cell lysates in presence of compound **62** as a proof for its target engagement with ME3 protein (**Figure 6.3**).

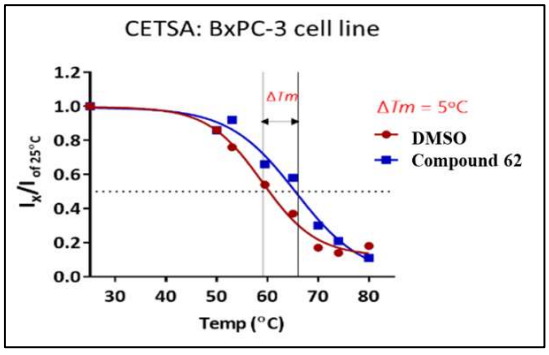

Figure 6.3: Melt-curve analysis for compound 62 with ME3 in BxPC-3 cells.

6.4.2.2 Isothermal Dose Response Fingerprint (ITDRF) study

A similar experiment was performed by pre-incubating various concentrations of compound **62** with BxPC-3 cell lysates at room temperature for 30 minutes, and then exposing them to 61°C; (a median temperature in the ΔT_m range, at which ME3 bound to 100 µM of compound **62** was found to be stable).

After performing the Western blot analysis, it was found that ME3 resisted temperature induced degradation at 61°C, in a concentration dependent manner of compound **62** (**Figure 6.4**). The EC_{50} of compound **62** for thermostabilization of ME3 was found to be 3.2 µM (**Figure 6.4**).

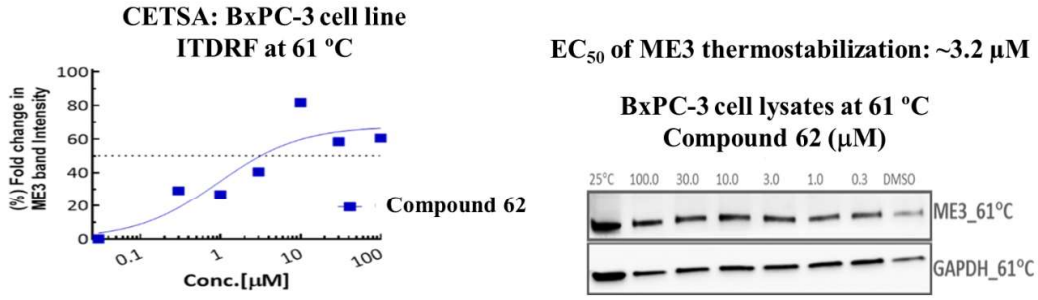

Figure 6.4: Isothermal Dose Response Fingerprint (ITDRF) with BxPC-3 cells

6.5 *in vitro* off target screening: Screening data for compound 31 to evaluate its safety in terms of off target side effects.

For safety pharmacology profiling, *in vitro* screening for compound **31** was carried out on 172 diverse proteins at 10 µM to evaluate its off target effects and results of this study is presented in **Table 6.3**.

Table 6.3: *in vitro* screening data for compound 31 with diverse protein targets

31

Sr. No.	Protein name	Species of origin	Concentration (μM)	Inhibition (%)
1	Adenosine A1	Human	10	0
2	Adenosine A2A	Human	10	0
3	Adenosine A2B	Human	10	0
4	Adenosine A3	Human	10	0
5	Adrenergic α1A	Human	10	6
6	Adrenergic α1B	human	10	5
7	Adrenergic α1D	human	10	0
8	Adrenergic α2A	human	10	0
9	Adrenergic α2B	human	10	0
10	Adrenergic α2C	human	10	0
11	Adrenergic β1	human	10	4
12	Adrenergic β2	human	10	0
13	Adrenergic β3	human	10	8
14	Aldosterone	human	10	0
15	Androgen (Testosterone)	human	10	0
16	Angiotensin AT1	human	10	8
17	Angiotensin AT2	human	10	9
18	APJ	human	10	16
19	Atrial Natriuretic Factor (ANF)	guinea pig	10	2
20	Bombesin BB1	human	10	0
21	Bombesin BB2	human	10	1
22	Bombesin BB3	human	10	1

Sr. No.	Protein name	Species of origin	Concentration (μM)	Inhibition (%)
23	Bradykinin B1	human	10	0
24	Bradykinin B2	human	10	0
25	Calcitonin	human	10	1
26	Calcitonin Gene-Related Peptide CGRP1	human	10	0
27	Calcium Channel L-Type, Benzothiazepine	rat	10	10
28	Calcium Channel L-Type, Dihydropyridine	rat	10	0
29	Calcium Channel L-Type, Phenylalkylamine	rat	10	0
30	Calcium Channel N-Type	rat	10	3
31	Cannabinoid CB1	human	10	19
32	Cannabinoid CB2	human	10	0
33	Chemokine CCR1	human	10	0
34	Chemokine CCR2B	human	10	0
35	Chemokine CCR5	rhesus macaque	10	0
36	Chemokine CX3CR1	human	10	0
37	Chemokine CXCR1 (IL-8RA)	human	10	3
38	Chemokine CXCR2 (IL-8RB)	human	10	16
39	Chemokine CXCR4	human	10	4
40	Cholecystokinin CCK1 (CCKA)	human	10	0
41	Cholecystokinin CCK2 (CCKB)	human	10	21
42	Colchicine	rat	10	6
43	Corticotropin Releasing Factor CRF1	human	10	0
44	CysLT2 (LTC4)	human	10	11

Sr. No.	Protein name	Species of origin	Concentration (μM)	Inhibition (%)
45	Dopamine D1	human	10	9
46	Dopamine D2S	human	10	8
47	Dopamine D3	human	10	0
48	Dopamine D4.4	human	10	3
49	Dopamine D5	human	10	0
50	Endothelin ETA	human	10	11
51	Endothelin ETB	human	10	2
52	Epidermal Growth Factor (EGF)	human	10	0
53	Estrogen ERα	human	10	49
54	Estrogen ERβ	human	10	13
55	GABAA, Chloride Channel, TBOB	rat	10	0
56	GABAA, Flunitrazepam, Central	rat	10	0
57	GABAA, Muscimol, Central	rat	10	11
58	GABAB1A	human	10	3
59	GABAB1B	human	10	0
60	Gabapentin	rat	10	3
61	γ-Hydroxybutyric Acid (GHB) Receptor	rat	10	0
62	Glucagon	human	10	0
63	Glucocorticoid	human	10	9
64	Glutamate, AMPA	rat	10	4
65	Glutamate, Kainate	rat	10	18
66	Glutamate, Metabotropic, mGlu2	human	10	8

Sr. No.	Protein name	Species of origin	Concentration (μM)	Inhibition (%)
67	Glutamate, Metabotropic, mGlu5	human	10	0
68	Glutamate, NMDA, Agonism	rat	10	0
69	Glutamate, NMDA, Glycine	rat	10	2
70	Glutamate, NMDA, Phencyclidine	rat	10	2
71	Glutamate, NMDA, Polyamine	rat	10	19
72	Glycine, Strychnine-Sensitive	rat	10	0
73	Gonadotropin-Releasing Hormone	human	10	0
74	Growth Hormone Secretagogue (GHS, Ghrelin)	human	10	0
75	Histamine H1	human	10	0
76	Histamine H2	human	10	1
77	Histamine H3	human	10	0
78	Histamine H4	human	10	0
79	Imidazoline I2, Central	rat	10	0
80	Inositol Trisphosphate IP3	rat	10	0
81	Insulin	rat	10	0
82	Interleukin IL-1 R1	human	10	5
83	Interleukin IL-6	human	10	0
84	IP (PGI2)	human	10	0
85	Leukotriene, BLT (LTB4)	human	10	0
86	Leukotriene, Cysteinyl CysLT1	human	10	0
87	Melanin-Concentrating Hormone MCH1 (SLC1)	human	10	0
88	Melanocortin MC1	human	10	0

Sr. No.	Protein name	Species of origin	Concentration (μM)	Inhibition (%)
89	Melanocortin MC3	human	10	6
90	Melanocortin MC4	human	10	0
91	Melanocortin MC5	human	10	0
92	Melatonin MT1	human	10	16
93	Melatonin MT2	human	10	19
94	Motilin	human	10	0
95	Muscarinic M1	human	10	2
96	Muscarinic M2	human	10	0
97	Muscarinic M3	human	10	0
98	Muscarinic M4	human	10	0
99	Muscarinic M5	human	10	0
100	Muscarinic, Oxotremorine M	rat	10	0
101	Neuropeptide Y Y1	human	10	0
102	Neuropeptide Y Y2	human	10	0
103	Neurotensin NT1	human	10	0
104	Nicotinic Acetylcholine α1, Bungarotoxin	human	10	10
105	Nicotinic Acetylcholine α3β4	human	10	0
106	Nicotinic Acetylcholine α4β2, Cytisine	rat	10	0
107	Nicotinic Acetylcholine α7, Bungarotoxin	rat	10	8
108	Nicotinic Acetylcholine α7, Methyllycaconitine	human	10	0
109	Opiate δ1 (OP1, DOP)	human	10	11
110	Opiate κ (OP2, KOP)	human	10	0

Sr. No.	Protein name	Species of origin	Concentration (μM)	Inhibition (%)
111	Opiate μ (OP3, MOP)	human	10	0
112	Orexin OX1	human	10	13
113	Orexin OX2	human	10	18
114	Orphanin ORL1	human	10	0
115	Oxytocin	human	10	7
116	Phorbol Ester	mouse	10	0
117	Platelet Activating Factor (PAF)	human	10	0
118	Platelet-Derived Growth Factor (PDGF)	mouse	10	3
119	Potassium Channel [KA]	rat	10	3
120	Potassium Channel [KATP]	Hamster	10	0
121	Potassium Channel [SKCA]	rat	10	0
122	Potassium Channel hERG	human	10	0
123	Progesterone PR-B	human	10	0
124	Prostanoid CRTH2	human	10	2
125	Prostanoid DP	human	10	2
126	Prostanoid EP1	human	10	5
127	Prostanoid EP2	human	10	0
128	Prostanoid EP3	human	10	0
129	Prostanoid EP4	human	10	22
130	Prostanoid FP	human	10	6
131	Purinergic P2X	rat	10	14
132	Purinergic P2Y, Non-Selective	rat	10	0

Sr. No.	Protein name	Species of origin	Concentration (μM)	Inhibition (%)
133	Retinoid X Receptor RXRα	human	10	2
134	Rolipram	rat	10	2
135	Ryanodine RyR3	rat	10	5
136	Serotonin (5-Hydroxytryptamine) 5-HT1A	human	10	8
137	Serotonin (5-Hydroxytryptamine) 5-HT1B	rat	10	0
138	Serotonin (5-Hydroxytryptamine) 5-HT2B	human	10	0
139	Serotonin (5-Hydroxytryptamine) 5-HT2C	human	10	0
140	Serotonin (5-Hydroxytryptamine) 5-HT3	human	10	0
141	Serotonin (5-Hydroxytryptamine) 5-HT4	guinea pig	10	14
142	Serotonin (5-Hydroxytryptamine) 5-HT5A	human	10	0
143	Serotonin (5-Hydroxytryptamine) 5-HT6	human	10	0
144	Serotonin (5-Hydroxytryptamine) 5-HT7	human	10	0
145	Sigma σ1	human	10	17
146	Sigma σ2	rat	10	30
147	Sodium Channel, Site 2	rat	10	13
148	Somatostatin sst1	human	10	0
149	Somatostatin sst2	human	10	2
150	Somatostatin sst3	human	10	4
151	Somatostatin sst4	human	10	0
152	Somatostatin sst5	human	10	0
153	Tachykinin NK1	human	10	0
154	Tachykinin NK2	human	10	4

Sr. No.	Protein name	Species of origin	Concentration (μM)	Inhibition (%)
155	Tachykinin NK3	human	10	0
156	Thyroid Hormone	rat	10	0
157	Thyrotropin Releasing Hormone (TRH)	human	10	0
158	Transforming Growth Factor-β (TGF-β)	mouse	10	3
159	Transporter, Adenosine	guinea pig	10	0
160	Transporter, Choline	rat	10	3
161	Transporter, Dopamine (DAT)	human	10	10
162	Transporter, GABA	rat	10	1
163	Transporter, Glycine	rat	10	0
164	Transporter, Norepinephrine (NET)	human	10	5
165	Transporter, Serotonin (5-Hydroxytryptamine) (SERT)	human	10	8
166	Transporter, Vesicular Monoamine (Non-selective)	human	10	22
167	Vasoactive Intestinal Peptide VIP1	human	10	0
168	Vasoactive Intestinal Peptide VIP2	human	10	0
169	Vasopressin V1A	human	10	3
170	Vasopressin V1B	human	10	14
171	Vasopressin V2	human	10	0
172	Vitamin D3	human	10	2

Compound **31** did not show notable inhibition of any of the diverse proteins included in the screening panel hence, it was confirmed to have a very good safety profile for pharmacological studies.

6.6 Antitumor activity of compound 31 in BxPC-3 subcutaneous (s.c.) xenograft in athymic nude mice

6.6.1 Brief protocol for *in vivo* study

i) 4-6 week old male athymic nude mice were subcutaneously injected in the flank region with 1 x 10^6 BxPC-3 cells (100 µL, 99.5% viability, passage no. 16) along with Matrigel in the final volume of 0.2 mL. Periodically, tumors were measured using Vernier Caliper till the tumor size reached in the range of 100-250 mm^3. Tumor-bearing mice were randomized into 6 treatment groups (n=4-7/group) based on their tumor volumes, such that mean tumor volume were similar across all the groups.

ii) PEG400 was added (20% of total volume) and vortexed thoroughly. Saline (60% of total volume) was added just prior to dosing while constantly vortexing the mixture. Vehicle formulation was prepared by using the same procedure as mentioned above, except addition of compound **31**.

iii) Nab-PTX and gemcitabine were prepared in saline. Compound **31** was administered daily while Nab-PTX and gemcitabine were administered once every four days, as per the study design described in **Table 6.4**. All the treatments were administered via intraperitoneal route.

Table 6.4: Treatment regime for compound 31, nab-PTX and gemcitabine

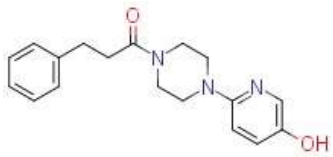

31

Group	Treatment	Dose (mg/kg)	Dosing Schedule	Conc. (mg/mL)	Dose Volume (mL/kg)	Treatment Period (Days)
1	Vehicle	-	i.p., OD	-	10	37
2	Compound **31**	50	i.p., OD	5.0	10	
3	Compound **31**	100	i.p., OD	10.0	10	
4	Compound **31**	200	i.p., OD	20.0	10	
5	Nab-PTX	20	i.p., O4D	2.0	10	
6	Gemcitabine	25	i.p., O4D	2.5	10	

OD-Once Daily; Q4D: once every four days; i.p.: Intraperitoneal

iv) Animals were monitored twice-in-a-week for tumor volume, body weight change and clinical signs. Tumor volume at subcutaneous implant site was estimated by twice-in-a-week measurements of the length and width of the tumor by electronic calipers and applying the equation: $V = L \times W^2/2$. The day of initiation of treatment was considered as day 1. Mice were euthanized by a slow CO_2 inhalation, when any signs of distress were observed. Signs of distress included loss of ambulation, labored breathing, or weight loss of >20% body weight of animal.

v) Tumor growth inhibition (%TGI) was calculated as [1-(average relative tumor volume treatment group/average relative tumor volume of vehicle group)] x 100. Tumor growth was analyzed by two-way ANOVA of matched values followed by Bonferroni multiple comparisons post hoc test to establish the significance between the groups at each day of treatment. Differences between groups were considered significant when the probability value (p) was ≤ 0.05. Statistical analysis was performed using GraphPad Prism 6.05 (San Diego, CA, USA).

vi) Schematic Diagram of Experiment Design:

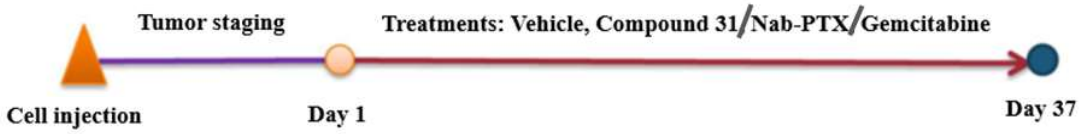

6.6.2 Results

i) Once daily administration of compound **31** at 50, 100 and 200 mpk, i.p. doses, showed anti-tumor activity against BxPC-3 xenograft in nude mice.

ii) The anti-tumor activity was statistically significant from day 16 onwards for 200 mpk dose and from day 23 onwards for 50 and 100 mpk dose groups for compound **31.**

iii) Nab-PTX at 20 mpk i.p. dose showed statistically significant anti-tumor effect from day 27 onwards. Gemcitabine at 25 mpk, i.p. dose did not show any significant effect.

iv) Results of tumor volume are presented in **Figure 6.5** and **Table 6.5**.

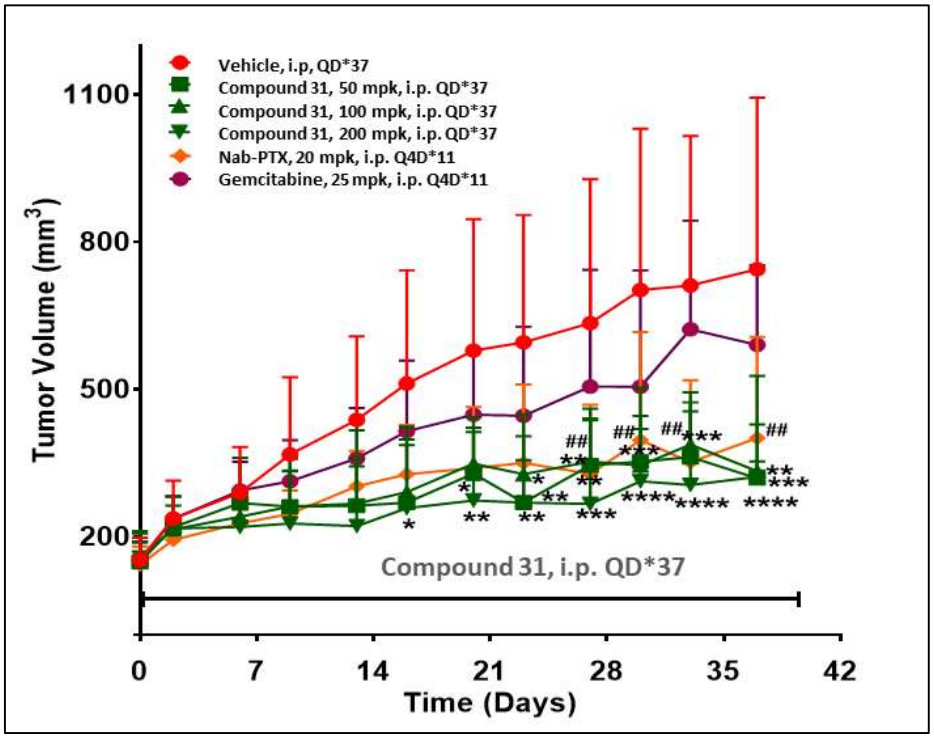

Figure 6.5. Growth inhibition of BxPC-3 xenografts in mice

Table 6.5: Anti-tumor effect of compound **31** in nude mice bearing BxPC-3 xenograft

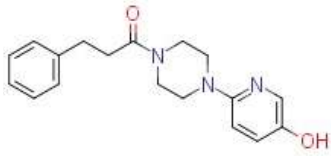

31

Treatment	Dose (mg/kg)	Route, Frequency	Mean Tumor Volume (mm^3) ± S.D.						
			0 day (Baseline)	2 day	6 day	9 day	13 day	16 day	20 day
Vehicle	-	i.p, OD	152.7 ± 45.1	237.1 ± 76.7	289.4 ± 93.0	367.5 ± 157.1	438.1 ± 169.9	511.9 ± 230.3	578.9 ± 267.7
Compound 31	50	i.p, OD	148.6 ± 39.3	219.4 ± 62.8	268.3 ± 92.2	261.2 ± 97.0	263.0 ± 153.8	269.6 ± 116.7	328.6 ± 114.8
Compound 31	100	i.p, OD	158.1 ± 48.3	214.7 ± 48.0	241.1 ± 46.2	261.6 ± 73.5	267.3 ± 91.1	291.0 ± 133.2	348.7 ± 64.3
Compound 31	200	i.p, OD	157.2 ± 53.7	216.6 ± 65.9	219.8 ± 75.4	226.7 ± 106.4	221.6 ± 121.6	257.9 ± 139.7*	273.7 ± 148.3**
Nab-PTX	20	i.p, O4D	143.0 ± 36.2	193.4 ± 44.4	227.1 ± 28.2	246.7 ± 47.0	302.8 ± 71.9	327.1 ± 100.3	339.8 ± 124.3
Gemcitabine	25	i.p, O4D	151.6 ± 38.4	236.2 ± 45.1	294.1 ± 58.6	312.7 ± 84.3	359.5 ± 102.5	414.7 ± 143.8	448.3 ± 131.3

Treatment	Dose (mg/kg)	Route, Frequency	Mean Tumor Volume (mm^3) ± S.D.					%TGI on Day 37
			23 day	27 day	30 day	33 day	37 day	
Vehicle	-	i.p, OD	595.6 ± 259.3	634.8 ± 293	702.1 ± 328.2	711.1 ± 304.6	744.5 ± 349.3	-
Compound 31	50	i.p, OD	269.6 ± 86.7**	345.2 ± 91.6*	352.7 ± 66.2**	362.0 ± 93.4**	318.6 ± 34.8***	48.5
Compound 31	100	i.p, OD	327.0 ± 122.1*	352.8 ± 88.2*	345.2 ± 101.0***	387.6 ± 106.1**	333.4 ± 94.9****	55.7
Compound 31	200	i.p, OD	269.2 ± 135.2**	267.0 ± 193.9***	312.9 ± 190.1***	305.3 ± 167.9****	321.5 ± 205.6****	62.0
Nab-PTX	20	i.p, O4D	350.2 ± 159.6	328.0 ± 140.7#	396.5 ± 219.8#	351.9 ± 166.6##	400.9 ± 205.8##	41.3
Gemcitabine	25	i.p, O4D	446.2 ± 181.6	505.4 ± 237.6	505.2 ± 236.5	622.6 ± 221.3	590.5 ± 162.0	17.3

Data are presented as mean ± SD, n=4-7/group, 2-way ANOVA followed by Bonferroni's post hoc test. *, #p< 0.05, **, ## p< 0.01, ***p<0.001. *Compared to vehicle control for compound 31, #compared to vehicle control for Nab-PTX.

6.7 Synergy study of compound 62 in combination with trametinib to assess synergistic effect on Hs766T cell growth inhibition.

6.7.1 Brief study protocol for combination study

Seeding of Hs766T cells was done as mentioned above in the short-term growth inhibition assay protocol. Next day, cells were treated with vehicle (0.5% DMSO) or a combination of trametinib and compound **62**. Both compounds were mixed and added to the cells to obtain their final concentrations as shown in **Table 6.6**.

Table 6.6: Concentrations of compound **62** and trametinib used for screening

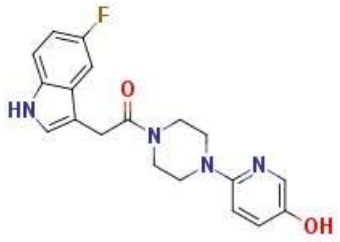

62

Compound 62 (µM)												
Trametinib (nM)					Compound 62 (µM) + Trametinib (nM)							
	1	2	3	4	5	6	7	8	9	10	11	12
A												

B		1.56	0.01	0.02	0.02 + 0.78	0.02 + 1.56	0.02 + 3.13	0.02 + 6.25	0.02 + 12.5	0.02 + 25	0.02 + 50	
C		3.13	100	0.10	0.10 + 0.78	0.10 + 1.56	0.10 + 3.13	0.10 + 6.25	0.10 + 12.5	0.10 + 25	0.10 + 50	
D		6.25	DMSO	0.39	0.39 + 0.78	0.39 + 1.56	0.39 + 3.13	0.39 + 6.25	0.39 + 12.5	0.39 + 25	0.39 + 50	
E		12.5	DMSO	1.6	1.6 + 0.78	1.6 + 1.56	1.6 + 3.13	1.6 + 6.25	1.6 + 12.5	1.6 + 25	1.6 + 50	
F		25	0.3125	6.25	6.25 + 0.78	6.25 + 1.56	6.25 + 3.13	6.25 + 6.25	6.25 + 12.5	6.25 + 25	6.25 + 50	
G		50	0.78	25	25 + 0.78	25 + 1.56	25 + 3.13	25 + 6.25	25 + 12.5	25 + 25	25 + 50	
H												

Duplicate plates were set up for each combination matrix and were incubated for 96 h, at 37ºC in 5% CO_2. Luminescence values were converted to percentage growth inhibition relative to the vehicle control (0.5% DMSO). IC_{50s} of trametinib were calculated in presence and absence of each concentration of compound **62** and vice versa, using GraphPad Prism software 9.04. The combination indices were calculated by Chou-Talalay's method and Loewe isobologram analysis of drug combination effect, using Combenefit® software.

The combination index (CI) was found to be < 1 indicating clear synergism between these two compounds (**Figure 6.6**).

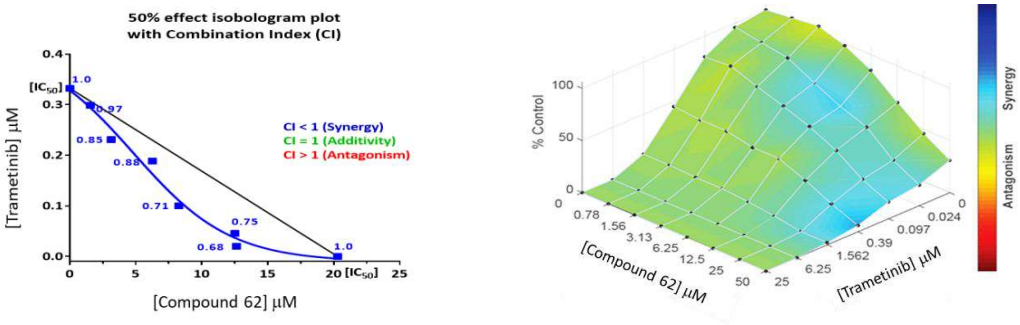

Figure 6.6. Combination index for compound 62 and trametinib

Overall summary and conclusion

- Compound **A** was identified as human ME3 inhibitor for the first time.
- Through systematic SAR study, structural attributes for potent and selective ME3 inhibitiors were identified
- Selective ME3 inhibitor, compound **31** was discovered and screened in vivo in BxPC-3 subQ xenograft model where it demonstrated significant TGI in comparison with current standard of care.
- Isobologram analysis of indole series compound **62** in combination with MEK inhibitor **trametinib** was performed for the first time where this combination showed synergistic effect on growth inhibition of Hs766T cells.
- Through investigation *in vitro* and *in vivo* studies, it was demonstrated that these compounds alone or in combination with other anti-cancer agents could be effective at killing PDAC cancer cells.
- These compounds may have therapeutic potential for the treatment of *SMAD4/ME2* null PDAC patients.